The Astrophysical Journal, 844:120 (7pp), 2017 August 1 https://doi.org/10.3847/1538-4357/aa7aac

Spectroscopy of 10 γ-Ray BL Lac Objects at High Redshift

Simona Paiano[1,2,3], Marco Landoni[3], Renato Falomo[1], Aldo Treves[4], and Riccardo Scarpa[5,6]
[1] INAF, Osservatorio Astronomico di Padova, Vicolo dell'Osservatorio 5, I-35122 Padova (PD), Italy
[2] Università di Padova and INFN, Via Marzolo 8, I-35131 Padova (PD), Italy
[3] INAF, Osservatorio Astronomico di Brera, Via E. Bianchi 46, I-23807 Merate (LC), Italy
[4] Università degli Studi dell'Insubria, Via Valleggio 11, I-22100 Como (CO), Italy
[5] Instituto de Astrofisica de Canarias, C/O Via Lactea, s/n E-38205 La Laguna (Tenerife), Spain
[6] Universidad de La Laguna, Dpto. Astrofísica, s/n E-38206 La Laguna (Tenerife), Spain
Received 2017 April 8; revised 2017 May 17; accepted 2017 May 18; published 2017 July 28

Abstract

We present optical spectra with high signal-to-noise ratio of 10 BL Lac objects detected at GeV energies by the *Fermi* satellite (3FGL catalog), which previous observations suggested are at relatively high redshift. The new observations, obtained at the 10 m Gran Telescopio Canarias, allowed us to find the redshift for J0814.5+2943 ($z = 0.703$), and we can set a spectroscopic lower limit for J0008.0+4713 ($z > 1.659$) and J1107.7+0222 ($z > 1.0735$) on the basis of Mg II intervening absorption features. In addition we confirm the redshifts for J0505.5 +0416 ($z = 0.423$) and J1450+5200 ($z > 2.470$). Finally we contradict the previous z estimates for five objects (J0049.7+0237, J0243.5+7119, J0802.0+1005, J1109.4+2411, and J2116.1+3339).

Key words: BL Lacertae objects: general – galaxies: distances and redshifts

Supporting material: data behind figure

1. Introduction

Blazars are active galactic nuclei (AGNs) where the relativistic jet is pointing in the observer's direction. They are characterized by high variability in all bands and large polarization. The spectral energy distribution (SED) exhibits two broad bumps, one in the IR–X-ray band and one in the MeV–TeV band. The former is due to synchrotron radiation produced by the relativistic electrons in the jet, while the latter in most models is due to the Compton scattering of the same electrons (e.g., Maraschi et al. 1992; Dermer & Schlickeiser 1993; Ghisellini & Tavecchio 2009). In some cases the thermal contribution due to the AGN accretion disk is also visible (see, e.g., Madejski & Sikora 2016 for a recent review).

Blazars are usually divided into two classes, BL Lac objects (BLLs) and flat-spectrum radio quasars (FSRQs), depending on the strength of the broad emission lines with respect to the continuum. A more physical distinction refers to the comparison between the luminosity of the broad-line region and the Eddington luminosity. FSRQs have radiatively efficient accretion disks, while BLLs are not able to photoionize gas in the clouds of the broad-line region, explaining the lacking of these features in the majority of their spectra (e.g., Ghisellini et al. 2017 and references therein). Note that this classification requires the knowledge of the mass of the accreting black hole, and of the distance, which can be easily determined by spectroscopy for AGNs with broad emission lines. However, this becomes arduous for the BLLs, due to the weakness of the spectral lines.

The advent of the *Fermi* gamma-ray observatory (1–100 GeV), which started observations in 2008 (Atwood et al. 2009) and systematically scans the entire sky every 3 hr, has substantially modified the study of blazars, which previously was based mostly on radio and X-ray surveys. In fact it was shown that blazars dominate the extragalactic gamma-ray sky (Acero et al. 2015). The third AGN *Fermi*/LAT catalog (3LAC, Ackermann et al. 2015) contains 1738 blazars, compared with the ~3000 γ-ray detected sources, where 662 are classified as BLL and 491 as FSRQ. The remaining blazars are reported as of uncertain type.

It is worth noting that the redshift of a large fraction of the BLLs is still unknown or highly uncertain. Based on the present statistics it was nevertheless proposed that on average BLLs have lower redshift and smaller high-energy (HE; >20 MeV) γ-ray luminosity than FSRQs (Ghisellini et al. 2017). This proposal, however, could be biased since at high redshift the number of robustly detected BLLs is drastically reduced due the difficulty of measuring the redshift (e.g., Falomo et al. 2014 and references therein). Moreover the uncertainty of the redshift makes it difficult to perform a sound comparison of the characteristics of the multiwavelength SED between the two classes of blazars, for which both the bolometric luminosity and redshift are needed (see the so-called *blazar sequence*, Fossati et al. 1998).

The determination of the redshift of BLLs is also important in order to characterize the properties of the extragalactic background light (EBL, e.g., Franceschini et al. 2008 and references therein). The very high-energy (VHE; >100 GeV) sky, observed with Cherenkov telescopes, is mainly dominated by BLLs (in the TeVcat[7] there are 60 BLLs against six FSRQs). Their energetic γ-rays can interact with lR–optical EBL photons to produce e^-/e^+ pairs, resulting in a clearly detectable absorption in the GeV–TeV BLL spectrum, starting at frequencies and with optical depth that depend on the redshift of the γ-ray source; this absorption is more pronounced in the interval $0.5 < z < 2$. At higher z the absorption due to pair production moves to *Fermi* energies, completely extinguishing the source in the VHE regime. Although a significant number of FSRQ detections already exist up to $z > 4$ (Ackermann et al. 2017), only a small fraction of them are detected at TeV energies, due to the position of their Compton inverse peak. Therefore it is particularly challenging to identify high-redshift[8]

[7] http://tevcat.uchicago.edu/
[8] Few known redshifts of BLLs range between 0.5 and 2.5.

Table 1
The Sample of 3FGL/LAC BL Lac Objects

3LAC Name	Other Name	R.A. (J2000)	δ (J2000)	V	$E(B-V)$ (mag)	Tentative Redshifts
3FGL J0008.0+4713	BZB J0007+4712	00:08:00.0	+47:12:08	18.30	0.08	0.28, 2.10
3FGL J0049.7+0237	PKS 0047+023	00:49:43.2	+02:37:04	18.00	0.01	1.44, 1.474
3FGL J0243.5+7119	BZB J0243+7120	02:43:30.9	+71:20:18	19.20	0.70	>0.998, ?
3FGL J0505.5+0416	BZB J0505+0415	05:05:34.8	+04:15:55	16.70	0.07	0.424, ?
3FGL J0802.0+1005	BZB J0802+1006	08:02:04.8	+10:06:37	17.42	0.02	0.842, ?
3FGL J0814.5+2943	EXO 0811+2949	08:14:21.3	+29:40:21	18.80	0.03	1.084
3FGL J1107.5+0222	BZB J1107+0222	11:07:35.9	+02:22:25	18.97	0.03	?
3FGL J1109.4+2411	1ES 1106+244	11:09:16.1	+24:11:20	18.70	0.02	0.482, 1.221
3FGL J1450.9+5200	BZB J1450+5201	14:50:59.9	+52:01:11	18.90	0.02	2.471, 2.474
3FGL J2116.1+3339	2FGL J2116+3339	21:16:14.5	+33:39:20	16.30	0.10	0.35, 1.596

Note. Column 1: 3FGL/LAC name of the target; Column 2: other name of the target; Column 3: R.A.; Column 4: decl.; Column 5: V-band magnitudes taken from the NASA/IPAC Extragalactic Database (NED); Column 6: $E(B-V)$ taken from the NASA/IPAC Infrared Science Archive (https://irsa.ipac.caltech.edu/applications/DUST/); Column 7: tentative redshift taken from the literature. For references see Plotkin et al. (2010), Shaw et al. (2013), 3LAC catalog (Ackermann et al. 2015), and NED.

Table 2
Log of GTC Observations of 3FGL/LAC BL Lac Objects

	Grism B				Grism R			
Object	$t_{\rm Exp}$ (s)	Date	Seeing ($''$)	r	$t_{\rm Exp}$ (s)	Date	Seeing ($''$)	r
3FGL J0008.0+4713	1800	2015 Oct 4	1.5	18.4	1800	2015 Nov 23	2.0	18.5
3FGL J0049.7+0237	3600	2015 Nov 23	1.5	18.5	3600	2015 Nov 23	1.9	18.5
3FGL J0243.5+7119	3600	2015 Nov 20	1.6	18.9	2700	2015 Nov 20	2.2	18.9
3FGL J0505.5+0416	3600	2016 Feb 5	1.1	16.9	3600	2016 Feb 5	1.1	16.9
3FGL J0802.0+1005	2100	2016 Jan 28	1.3	18.5	2100	2016 Jan 28	1.3	18.5
3FGL J0814.5+2943	3600	2016 Feb 6	1.3	18.3	3600	2016 Feb 6	1.3	18.3
3FGL J1107.5+0222	3000	2015 Dec 23	1.6	18.3	3000	2015 Dec 23	1.9	18.3
3FGL J1109.4+2411	3600	2016 Jan 28	1.0	17.8	3600	2016 Jan 21	0.9	18.0
3FGL J1450.9+5200	1500	2015 Mar 14	2.2	18.4	1800	2015 Mar 14	2.1	18.4
3FGL J2116.1+3339	450	2015 Dec 24	1.9	16.7	450	2015 Dec 24	1.9	16.7

Note. Column 1: name of the target; Column 2: total integration time with grism B; Column 3: date of observation with grism B; Column 4: seeing during the observation with grism B; Column 5: r ABmag measured on the acquisition image for grism B; Column 6: total integration time with grism R; Column 7: date of observation with grism R; Column 8: seeing during the observation with grism R; Column 9: r ABmag measured on the acquisition image for grism R.

BLLs at these energies in order to study the earliest EBL components due to the first-light sources (Population III stars, galaxies, or quasars) in the universe (Franceschini & Rodighiero 2017).

In the framework of our long-term optical spectroscopy program at large (8–10 m) telescopes, aimed at determining the redshift of the BLLs (Sbarufatti et al. 2005, 2006; Landoni et al. 2012, 2013, 2014, 2015; Sandrinelli et al. 2013; Paiano et al. 2016, 2017), we concentrate here on 10 BLLs detected by the *Fermi* satellite with unknown or very uncertain redshift.

In this work we assume the following cosmological parameters: $H_0 = 70$ km s^{-1} Mpc^{-1}, $\Omega_\Lambda = 0.7$, and $\Omega_m = 0.3$.

2. Sample, Reduction, and Data Analysis

We searched for BLLs that are candidates for being at high redshift ($z > 1$) in the *Fermi* 3LAC catalog. These objects have uncertain redshift, and in most cases conflicting values are reported in the literature, mainly due to spectra with low signal-to-noise ratio (S/N). Considering only the sources that can be well observed from the La Palma site, the selection produced 18 targets and we obtain observations for 10 of them (see Table 1).

The observations were gathered in Service Mode at the Gran Telescopio Canarias (GTC) using the low-resolution spectrograph OSIRIS (Cepa et al. 2003). The instrument was configured with the grisms R1000B and R1000R[9] in order to cover the whole spectral range 4100–10000 Å, and with a slit width = 1″ yielding a spectral resolution $\lambda/\Delta\lambda = 800$.

For each grism, we obtained three individual exposures (with exposure time ranging from 150 to 1200 s each, depending on the source magnitude), which were combined into a single average image, in order to perform an optimal cleaning of cosmic rays and CCD cosmetic defects. Wavelength calibration was performed using the spectra of Hg, Ar, Ne, and Xe lamps and provided an accuracy of 0.1 Å over the whole spectral range. For each object the spectra obtained with the two grisms were merged into a final spectrum covering the whole desired spectral range. Spectra were corrected for atmospheric extinction using the table of mean extinction for the La Palma site.[10] Relative flux calibration was provided by spectrophotometric standard stars secured during the same nights as the target exposure. The observation strategy and the data reduction

[9] http://www.gtc.iac.es/instruments/osiris/osiris.php
[10] https://www.ing.iac.es/Astronomy/observing/manuals/

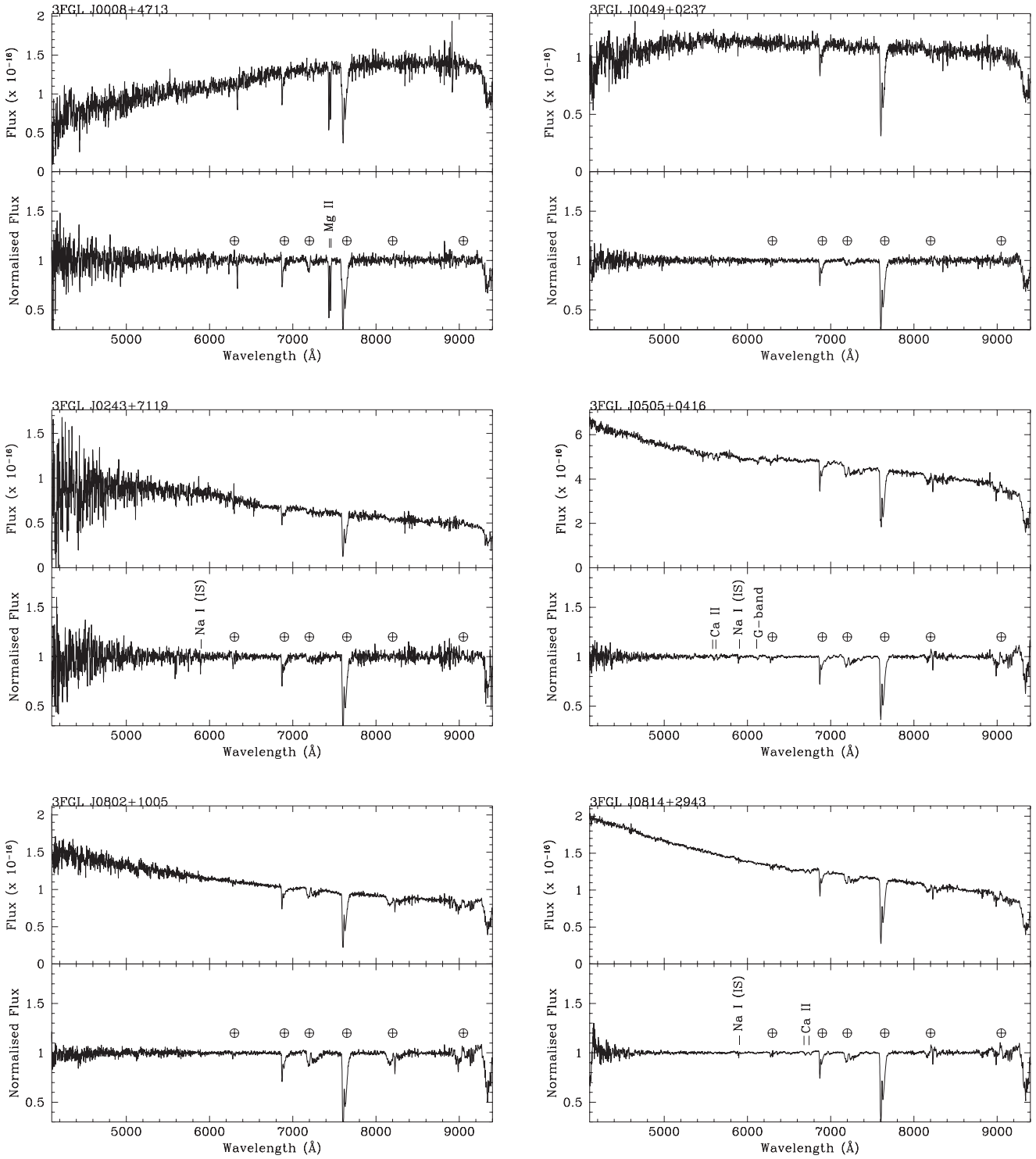

Figure 1. Spectra of the high-redshift 3FGL/LAT BLLs obtained at GTC. Top panels: flux-calibrated and dereddened spectra. Bottom panels: normalized spectra. The main telluric bands are indicated by ⊕, the absorption features from the interstellar medium of our galaxies are labelled as IS. The data used to create this figure are available

followed the procedure reported in Paiano et al. (2017) and detailed information on the observations is given in Table 2.

3. Results

The optical spectra of the targets are presented in Figure 1. In order to emphasize weak emission and/or absorption features, we show also the normalized spectrum. This was obtained by dividing the observed calibrated spectrum by a power-law continuum fit of the spectrum, excluding the telluric absorption bands (see Table 3). The normalized spectra were used to evaluate the S/N in a number of different spectral regions. On average, the S/N ranges from 10 to 200 depending on the wavelength and the magnitude of the source (Table 3). These

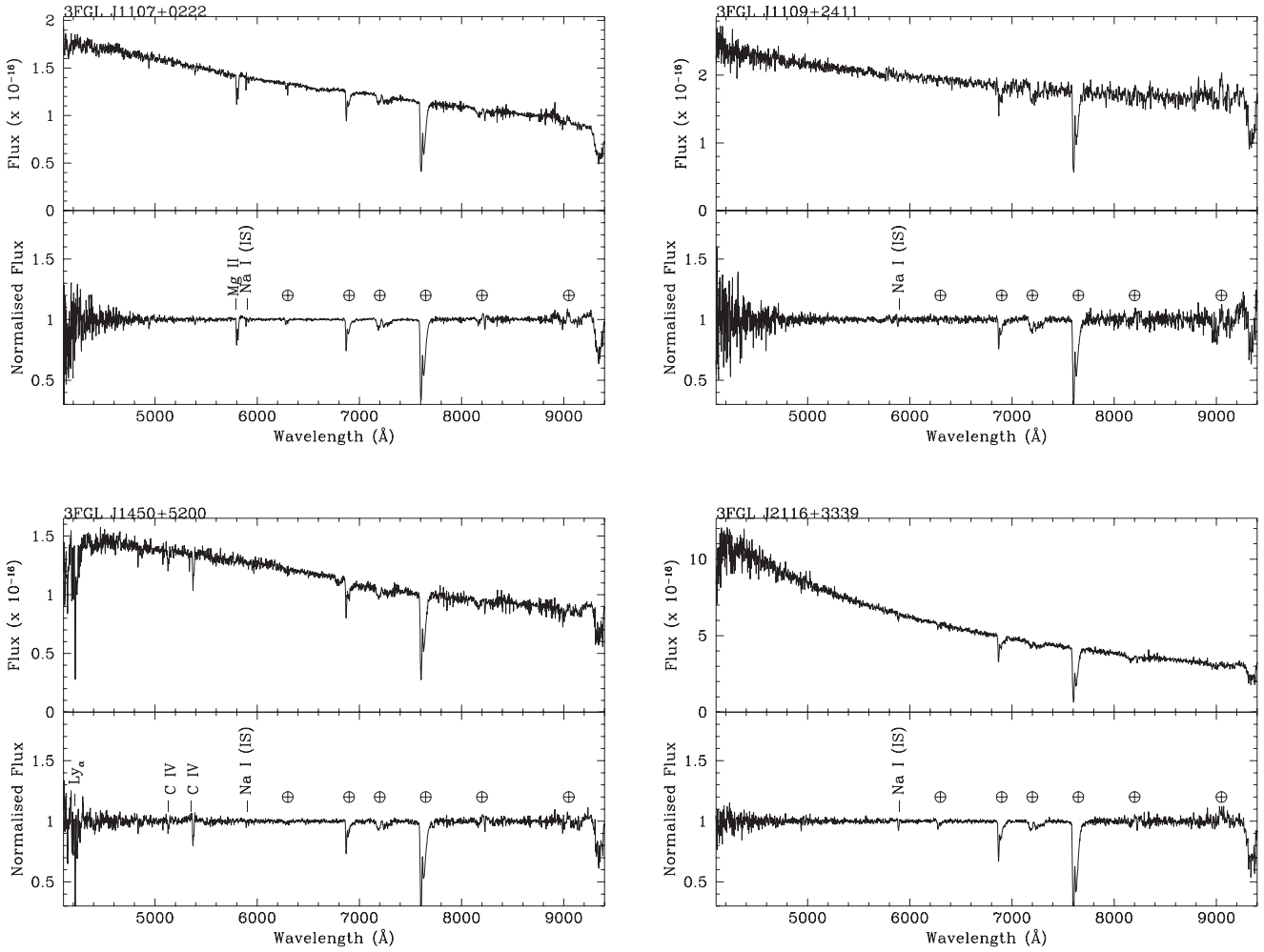

Figure 1. (Continued.)

Table 3
Properties of the Optical Spectra of 3FGL/LAC Sources

Object	α	S/N	EW_{min}	z
3FGL J0008.0+4713	+0.74*	10–50	0.50–3.10	>1.659[i]
3FGL J0049.7+0237	−0.01	27–95	0.30–1.20	>0.55[ll]
3FGL J0243.5+7119	−0.95	10–65	0.45–3.25	>0.45[ll]
3FGL J0505.5+0416	−0.62	40–150	0.15–0.65	0.423[g]
3FGL J0802.0+1005	−0.77	32–108	0.30–0.70	>0.58[ll]
3FGL J0814.5+2943	−0.95	54–161	0.20–0.55	0.703[g]
3FGL J1107.5+0222	−0.82	27–208	0.15–1.15	>1.0735[i]
3FGL J1109.4+2411	−0.50	22–71	0.35–1.15	>0.50[ll]
3FGL J1450.9+5200	−0.73	32–119	0.25–1.00	>2.470[i]
3FGL J2116.1+3339	−1.66	40–130	0.30–0.85	>0.25[ll]

Note. Column 1: name of the target; Column 2: optical spectral index derived from a power-law fit in the range 4250–10000 Å; Column 3: range of S/N of the spectrum; Column 4: range of the minimum equivalent width (EW_{min}) derived from different regions of the spectrum (see text), Column 5: redshift proposed in this work. The superscript letters indicate g—host galaxy absorption, i—intervening absorption, ll—lower limit of the redshift by assuming a BL Lac host galaxy with $M_R = -22.9$.

spectra can be accessed at the website http://www.oapd.inaf.it/zbllac/.

All spectra were carefully inspected to find emission and absorption features. When a possible feature was identified, we determined its reliability by checking that it was present in the three individual exposures (see Section 2 for details).

We were able to detect stellar spectral features of Ca II ($\lambda\lambda$3934, 3968) for 3FGL J0505.5+0416 and 3FGL J0814.5+2943. For two sources, 3FGL J0008.0+4713 and 3FGL J1107.5+0222, we detect a strong intervening absorption system due to Mg II (λ2800), allowing us to set a spectroscopic lower limit on their redshift. Finally in one object, 3FGL 1450.9+5200, we detect intervening absorption systems due to C IV (λ1548) and Lyα (λ1216) at two different redshifts. For five other objects the spectrum appears featureless in contrast with the previously claimed redshift values. Details are reported in Figure 2 and Table 4.

Starting from the basic assumption that all BLLs are hosted by a massive elliptical galaxy, one is able to detect faint absorption features from the starlight, provided that the S/N and the spectral resolution are sufficiently high. According to the scheme outlined in Paiano et al. (2017), in the case of no detection of spectral features it is also possible to set a lower limit to the redshift based on the minimum equivalent width (EW) of the spectrum (see Appendix A of Paiano et al. 2017 for details). The results for the redshift lower limits obtained for the whole sample are summarized in Table 3 and details about the optical spectra and redshift estimates for each individual object of our sample are given in Section 4.

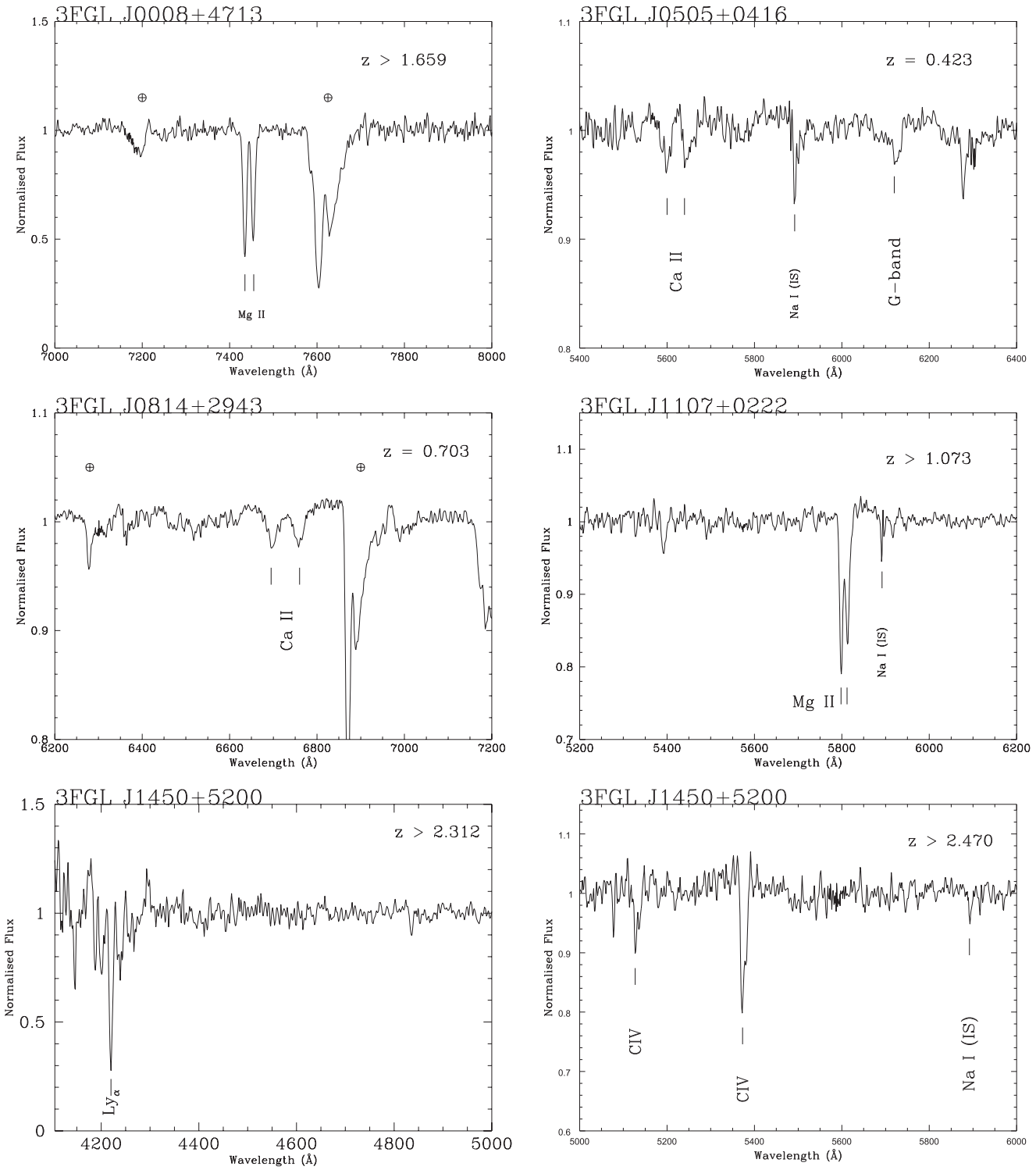

Figure 2. Close-up of the normalized spectra around the detected spectral features of the high-redshift 3FGL/LAT BLLs obtained at GTC. Main telluric bands are indicated by ⊕; spectral lines are marked by line identification.

4. Notes for Individual Sources

3FGL J0008.0+4713. A redshift of 0.28 was proposed from an optical spectrum provided by Kock et al. (1996), based on absorption features of its host galaxy (the spectrum is not published). However, the object appears unresolved in optical images (Nilsson et al. 2003). A more recent and rather noisy spectrum from Shaw et al. (2013) gives a tentative high redshift of $z = 2.1$, based on the onset of the Lyα forest. In our spectrum we clearly detect an intervening absorption doublet at 7440 Å (see Table 4) that we identify with Mg II (λ2800) at $z = 1.659$. No other emission or absorption features are found. The continuum is well fitted by a power law with a rather flat spectral index ($\alpha = +0.74$, $F_\nu \propto \nu^\alpha$), suggesting dust extinction possibly associated with

Table 4
Measurements of Spectral Lines

Object	λ_{obs} (Å)	EW (observed) (Å)	Line ID	z_{line}
3FGL J0008.0+4713	7434.94	5.3	Mg II (λ2796)	1.659
	7454.20	4.2	Mg II (λ2803)	1.659
3FGL J0505.5+0416	5598.08	0.8	Ca II (λ3934)	0.423
	5646.46	0.6	Ca II (λ3968)	0.423
	6126.02	0.7	G-band (λ4305)	0.423
3FGL J0814.5+2943	6699.60	0.6	Ca II (λ3934)	0.703
	6757.50	0.5	Ca II (λ3968)	0.703
3FGL J1107.5+0222	5797.50	2.0	Mg II (λ2796)	1.0735
	5812.02	1.9	Mg II (λ2803)	1.0735
3FGL J1450.9+5200	4219.69	5.8	Ly α (λ1216)	2.470
	5127.64	1.1	C IV (λ1548)	2.312
	5372.25	3.2	C IV (λ1548)	2.470

Note. `Column 1`: name of the target; `Column 2`: barycenter of the detected line; `Column 3`: measured equivalent width; `Column 4`: line identification; `Column 5`: spectroscopic redshift.

intervening gas at $z = 1.659$. This target is therefore one of the highest redshift BLLs known thus far.

3FGL J0049.7+0237. The first optical spectrum was secured by Dunlop et al. (1989), who found the source to be featureless. The same result was obtained a few years later by Allington-Smith et al. (1991). A superior quality optical spectrum was then published by Sbarufatti et al. (2006) that confirmed the featureless spectrum of the source, while Shaw et al. (2013) claim the detection of broad emission at ~ 6930 Å identified as Mg II (λ2800), suggesting $z = 1.474$. From our spectrum ($S/N \sim 100$), we contradict the presence of the above feature, and therefore the redshift is still unknown. We set a lower limit based on the nondetection of the starlight (see Section 3) of $z > 0.55$.

3FGL J0243.5+7119. A featureless optical spectrum was reported by Stickel & Kuehr (1996). A possible intervening absorption of Mg II (λ2800) at 5595 Å is claimed by Shaw et al. (2013), yielding a redshift limit of $z > 1$. We do not confirm this absorption doublet in our spectrum and note that at this wavelength there is a very strong night-sky emission. We also note that this source is at low Galactic latitude ($b = 10°$) and therefore the source is severely absorbed ($E(B - V) = 0.7$). We set a lower limit of $z > 0.45$ based on the lack of starlight features.

3FGL J0505.5+0416. This is a radio source (Bennett et al. 1986; Bauer et al. 2000) well detected at X-ray and gamma-ray frequencies (Voges et al. 1999; Acero et al. 2015). The first optical spectrum is reported in Laurent-Muehleisen et al. (1998) and fails to detect any lines. Optical images, obtained by Nilsson et al. (2003), were able to resolve the host galaxy, indicating a relatively low redshift. The optical spectrum obtained by Pita et al. (2014) shows absorption features of the host galaxy, yielding a redshift of 0.424. We confirm the Ca II doublet ($\lambda\lambda$3934, 3968), which in the spectrum of Pita et al. (2014) was in the merging region of the UVB and VIS arms of the instrument, and we also detect the absorption line due to the G-band (λ4305) at $z = 0.423$ (see Figure 2).

3FGL J0802.0+1005. The object was identified as a BLL by Plotkin et al. (2010) on the basis of the spectrum from the Sloan Digital Sky Survey (SDSS); it is not yet detected in the X-ray band and the counterpart is very faint in the radio regime (Condon et al. 1998). It was observed twice by SDSS, and two different redshifts were proposed from the automatic line identification ($z = 0.06$ and $z = 0.842$). Our visual inspection of these two spectra shows no significant presence of emission or absorption lines. Our optical spectrum confirms the featureless continuum described by a power law of $\alpha = -0.77$, and we can set a relatively high redshift limit of $z > 0.58$.

3FGL J0814.5+2943. White et al. (2000) found a featureless optical spectrum. With our high $S/N \sim 160$, we detect an absorption doublet system at 6699–6759 Å that we identify as Ca II at $z = 0.703$ from the starlight of the host galaxy (see Figure 2). We note that the redshift value reported by NED ($z = 1.083$) based on the SDSS spectrum is contradicted by our spectrum.

3FGL J1107.5+0222. Plotkin et al. (2010) found a featureless optical spectrum based on SDSS data. We clearly detect an absorption doublet at 5797, 5812 Å that we identify with an Mg II (λ2800) intervening system at $z = 1.0735$ (see Figure 2).

3FGL J1109.4+2411. The source was discovered and identified as a BLL by the X-ray Einstein Sky Survey (Perlman et al. 1996). The host galaxy was detected from snapshot images from the *Hubble Space Telescope*, suggesting a redshift $z \sim 0.5$ (Falomo & Kotilainen 1999; Sbarufatti et al. 2005). The optical spectrum obtained by SDSS is found to be featureless[11] (Shaw et al. 2013) and a spectrum from the ESO's Very Large Telescope reported by Landoni et al. (2013) also appears to be featureless. We obtain an optical spectrum with an S/N ranging from 20 to 70, and no significant emission or absorption lines are detected with a minimum EW of $\sim$0.35 Å, which allows us to set a redshift lower limit of $>$0.5.

3FGL J1450.9+5200. The source was proposed as a very high-redshift BLL by Plotkin et al. (2010) on the basis of intervening absorption of C IV(λ1548) and Lyα (λ1216) in the SDSS spectrum at a redshift of $z = 2.474$. We also detect the presence of the absorption line at 5372 Å identified as C IV (λ1548) intervening gas, and at the same redshift we see a strong Ly α (λ1216) absorption. In addition, we find an absorption feature at 5127 Å, which we interpret as a second

[11] The SDSS automatic line identification gives $z = 1.22$.

C IV (λ1548) intervening system at $z = 2.312$. Finally other absorption lines due to Ly α are observed at $\lambda < 4219$ Å. The redshift of this source is thus $z > 2.474$.

The source is detected by *Fermi* up to the interval 60–80 GeV (The Fermi-LAT Collaboration 2017). The optical depth at $z = 2.470$ for pair production in the EBL is $\tau \sim 1$ (see Figure 10 of Franceschini & Rodighiero 2017). *3FGL J2116.1+3339*. The source was originally detected in the radio band (B2114+33) and it appears in ROMA BZCAT (BZB J2116+3339, Massaro et al. 2015), which reports radio, optical ($R = 15.4$), X-ray, and gamma-ray fluxes. An optical spectrum is given by Shaw et al. (2013), which to us appears featureless, although the authors claim a redshift of 1.596 based on a very dubious, extremely faint C IV (λ1548) emission. In contrast, we do not detect any emission or absorption lines with EW > 0.30 Å in our spectrum, and we set a redshift lower limit of >0.25.

5. Conclusion

The discovery of hundreds of BLLs by the *Fermi* satellite motivates accurate optical spectroscopic studies, which in most cases require the use of large telescopes. In fact, the information on the redshift derives from the detection of very weak absorption or emission lines, at the source or in the intervening material. Our paper has focused on 10 sources detected at GeV energies, for which we present spectra of very good quality with S/N values ranging up to ~200. They were chosen from among objects already observed with smaller telescopes or with a poor S/N spectrum, and there was some indication that they were at relatively high z. Spectral features were detected for five out of 10 sources studied, while for the rest the only information on the redshift is a lower limit based on the absence of absorption lines from the host galaxy. For eight out of the 10 sources the redshifts are above 0.5, and two of them are two of the farthest BLLs yet known, 3FGL J0008.0+4713 ($z > 1.659$) and 3FGL J1450.9+5200 ($z > 2.470$). In spite of the improvement in the observing facilities (large telescope and modern instrumentation), determination of the redshift of some high-redshift BLLs remains rather arduous. However, this knowledge is crucial to advancing of our understanding of BLLs in a cosmic context.

References

Acero, F., Ackermann, M., Ajello, A., et al. 2015, ApJS, 218, 23
Ackermann, M., Ajello, M., Atwood, W. B., et al. 2015, ApJ, 810, 14
Ackermann, M., Ajello, M., Baldini, L., Ballet, J., & Barbiellini, G. 2017, ApJL, 837, L5
Allington-Smith, J. R., Peacock, J. A., & Dunlop, J. S. 1991, MNRAS, 253, 287
Atwood, W. B., Abdo, A. A., Ackermann, M., et al. 2009, ApJ, 697, 1071
Bauer, F. E., Condon, J. J., Thuan, T. X., & Broderick, J. J. 2000, ApJS, 129, 547
Bennett, C. L., Lawrence, C. R., Burke, B. F., Hewitt, J. N., & Mahoney, J. 1986, ApJS, 61, 1
Cepa, J., Aguiar-Gonzalez, M., Bland-Hawthorn, J., et al. 2003, Proc. SPIE, 4841, 1739
Condon, J. J., Cotton, W. D., Greisen, E. W., et al. 1998, AJ, 115, 1693
Dermer, C. D., & Schlickeiser, R. 1993, ApJ, 416, 458
Dunlop, J. S., Peacock, J. A., Savage, A., et al. 1989, MNRAS, 238, 1171
Falomo, R., & Kotilainen, J. K. 1999, A&A, 352, 85
Falomo, R., Pian, E., & Treves, A. 2014, A&ARv, 22, 73
Fossati, G., Maraschi, L., Celotti, A., Comastri, A., & Ghisellini, G. 1998, MNRAS, 299, 433
Franceschini, A., & Rodighiero, G. 2017, A&A, 603, A34
Franceschini, A., Rodighiero, G., & Vaccari, M. 2008, A&A, 487, 837
Ghisellini, G., Righi, C., Costamante, L., & Tavecchio, F. 2017, MNRAS, 469, 255
Ghisellini, G., & Tavecchio, F. 2009, MNRAS, 397, 985
Kock, A., Meisenheimer, K., Brinkmann, W., Neumann, M., & Siebert, J. 1996, A&A, 307, 745
Landoni, M., Falomo, R., Treves, A., et al. 2012, A&A, 543, A116
Landoni, M., Falomo, R., Treves, A., et al. 2013, AJ, 145, 114
Landoni, M., Falomo, R., Treves, A., & Sbarufatti, B. 2014, A&A, 570, A126
Landoni, M., Falomo, R., Treves, A., Scarpa, R., & Reverte Payá, D. 2015, AJ, 150, 181
Laurent-Muehleisen, S. A., Kollgaard, R. I., Ciardullo, R., et al. 1998, ApJS, 118, 127
Madejski, G., & Sikora, M. 2016, ARA&A, 54, 725
Maraschi, L., Ghisellini, G., & Celotti, A. 1992, ApJL, 397, L5
Massaro, E., Maselli, A., Leto, C., et al. 2015, Ap&SS, 357, 75
Nilsson, K., Pursimo, T., Heidt, J., et al. 2003, A&A, 400, 95
Paiano, S., Landoni, M., Falomo, R., et al. 2017, ApJ, 837, 144
Paiano, S., Landoni, M., Falomo, R., Scarpa, R., & Treves, A. 2016, MNRAS, 458, 2836
Perlman, E. S., Stocke, J. T., Schachter, J. F., et al. 1996, ApJS, 104, 251
Pita, S., Goldoni, P., Boisson, C., et al. 2014, A&A, 565, A12
Plotkin, R. M., Anderson, S. F., Brandt, W. N., et al. 2010, AJ, 139, 390
Sandrinelli, A., Treves, A., Falomo, R., et al. 2013, AJ, 146, 163
Sbarufatti, B., Treves, A., & Falomo, R. 2005, ApJ, 635, 173
Sbarufatti, B., Treves, A., Falomo, R., et al. 2006, AJ, 132, 1
Shaw, M. S., Romani, R. W., Cotter, G., et al. 2013, ApJ, 764, 135
Stickel, M., & Kuehr, H. 1996, A&AS, 115, 1
The Fermi-LAT Collaboration 2017, arXiv:1702.00664
Voges, W., Aschenbach, B., Boller, T., et al. 1999, A&A, 349, 389
White, R. L., Becker, R. H., Gregg, M. D., et al. 2000, ApJS, 126, 133